J. Chem. Sci. Vol. 127, No. 11, November 2015, pp. 1993–2003.
DOI 10.1007/s12039-015-0970-3

Preparation of Poly(MA-*alt*-α-olefin-$C_{6,8,12,18}$)/Silica Nanohybrids *via in situ* generated nanofillers for use as a dual function organonanofiller

DENİZ DEMİRCAN[a,*], GÜNAY KİBARER[a] and ZAKİR M O RZAYEV[b]
[a]Department of Chemistry, Hacettepe University, 06800 Ankara, Turkey
[b]The Institute of Science & Engineering, Division of Nanotechnology and Nanomedicine, Hacettepe University, 06800 Ankara, Turkey
e-mail: demircan@hacettepe.edu.tr

MS received 15 August 2014; revised 16 July 2015; accepted 1 September 2015

Abstract. Four types of copolymer-silica nanocomposites have been prepared via ring-opening grafting of γ-aminopropyltrimethoxysilane (APTS) as reactive coupling agent onto preformed copolymers of maleic anhydride (MA) with 1-hexene, 1-octene, 1-dodecene and 1-octadecene and *in situ* hydrolysis (polycondensation) of side-chain ethoxysilane groups and tetraethoxysilane as a precursor in the presence of HCl catalyst. The copolymers of MA with 1-hexene, 1-octene and 1-dodecene were synthesized by free radical polymerization and another MA copolymer with 1-octadecene was supplied commercially as matrix copolymer. Chemical/physical structures, thermal behavior and morphology investigations of the generated hybrids were performed by FTIR, ^{13}C, ^{29}Si-NMR, TGA, SEM and TEM analysis methods. Nano-level hybridization through covalent bonding (amidization) between the anhydride unit of copolymers and amine group of APTS was observed, and nanosilica networks (hydrolysis) were obtained through acid catalyzed co-polycondensation of TEOS and ethoxysilane fragments from both coupling agent and precursor. Agreeing with ^{29}Si-NMR and TGA quantitative analysis results, the degree of hydrolysis of ethoxysilane groups varied from 51.0 to 60.9%, and the content of *in situ* generated silica particles was found to be around 70.7-75.7%. Thermal properties and thermal stability of the obtained hybrids were found to be enhanced with silica content. SEM analysis confirmed the formation of nanostructural hybrids with relatively fine distributed nanoparticles. TEM analyses of all the nanohybrids indicate the formation of spherical morphologies. These novel copolymer hybrids are expected to be a promising and efficient organonanofiller for the preparation of polymer nanocomposites with both dual functionality and compatibilizer effects.

Keywords. Polymer-silica nanohybrids; ^{29}Si-NMR; thermal analysis; TEOS; SEM; TEM.

1. Introduction

In recent years, organic-inorganic polymer hybrids with a large variety of functionality have been studied intensively. Organic–inorganic hybrid materials are designed to achieve the maximum possible enhancement of properties including improved physical, mechanical and thermal properties for macromolecular materials through the *in situ* formation of nanostructured inorganic oxide domains. These materials have evolved from the sol-gel technology used for the production of ceramic coatings, powders, and fibers.[1] These new hybrid materials possess a controllable combination of the properties of both organic polymers and inorganic glasses.[2]

The sol–gel process is one of the most suitable methods to prepare silica gel through Si–O–Si linkages by the hydrolysis of alkoxysilanes. The polymer hybrids were prepared by reacting tetraalkoxysilanes with organic polymer through sol–gel process.[3] The properties of organic–inorganic hybrid materials highly depend on the interaction between the organic polymers and the siloxane matrix[4] and their homogeneous distribution within the hybrid systems. The concept of *in situ* generated fillers is derived from the fact that the inorganic phase is produced during processing, unlike in the case of conventional fillers, which are added as pre-formed particles, even though these may also have been produced by the sol-gel method.[5] The *in-situ* development of a three-dimensional cross-linked inorganic network structure using an organic precursor such as an alkoxide, $M(OR)_4$, can be carried out within the polymer matrix. The hydrolysis and condensation reactions involved in the process may proceed as follows (figure 1).[6]

Covalent bond formation decreases the extent of phase separation and increases the compatibility of organic and inorganic phases. One route can be given

*For correspondence

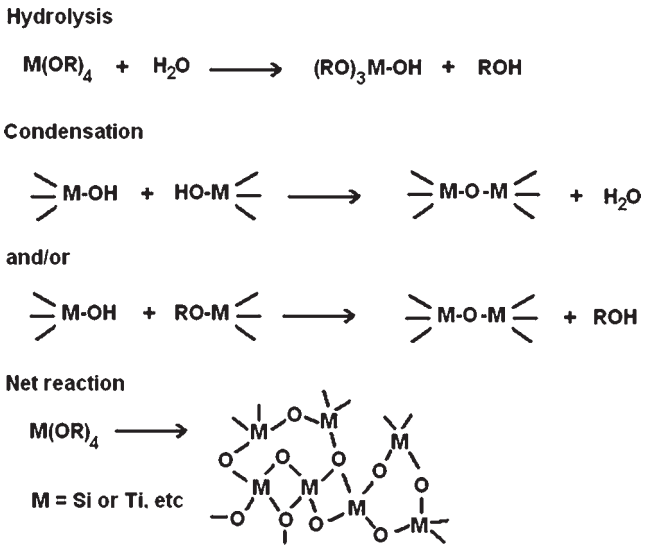

Figure 1. The hydrolysis and condensation reactions for *in situ* sol-gel process.

from the reference concerning a P(St-*co*-MA)/SiO_2 hybrid material,[7] prepared through which the alternating copolymerization of styrene and maleic anhydride proceed in the presence of (3-glycidoxypropyl) trimeyhoxysilane. They found the maximal content of SiO_2 in the resulting hybrid materials as being limited to a rather low value, mostly, due to the absence of TEOS. Consequently, in order to obtain a higher SiO_2 composition, an inorganic precursor (TEOS) was successfully employed in this work.

Polyolefins are a very important class of commercial polymers in the world today and are used in a wide spectrum of applications.[8,9] Despite their versatility, they suffer from certain drawbacks that exert a limiting influence on the range of applications. They are nonpolar and therefore exhibit poor hygroscopicity, printability and dyability. In addition, they have poor dispersibility with inorganic fillers like talc and mica in composites and poor miscibility in blends, even with themselves and alloys, with polymers like nylons, polyesters, engineering thermoplastics and so forth.[10] This restricts their use in several new emerging technologies. There is a report for a polyolefin-clay hybrid prepared by using a functional oligomer as a compatibilizer. They prepared PP–clay hybrids using a MA-modified PP oligomer as a compatibilizer and studied the dispersibility of clays. Until then, there was no report for the preparation of polyolefin–clay hybrids in literature when Hasegawa *et al.*[8] reported this novel approach. Recently, we have successfully prepared some poly(MA-*alt*-α-olefin)/organoclay nanocomposites for which the restricting effects on the combination of olefin copolymers and clays were eliminated by selecting appropriate copolymer systems with dual functionality.[11]

In regard to these facts mentioned in the above study, we selected our system in a way to obtain a combo-organonanofiller combining both organo-functionality and compatibilizer effect in one product. For this purpose, we synthesized MA copolymers with four different olefins containing both reactive and functional groups, having the ability to interact with both inorganic coupling agents (functionalized conventionally) and long/branched alkyl chains, thus, resulting in an organofiller compound quite compatible with polyolefin copolymers.

MA is known to form an alternating copolymer with electron-donor heterocyclic monomers. The formation of a charge transfer complex (CTC) in MA-donor monomer systems was observed and complex-radical copolymerization of MA with various electron-donor functional monomers was achieved.[12] Such a copolymer is formed independent of the initial ratio of the comonomers.[13] The free radical copolymerization of maleic anhydride with propylene and higher olefins was investigated by Frank[14]; in all cases, copolymers with alternating structure were obtained. In previous studies,[15] molar mass of MA copolymers with long-chain α-olefins (C_6, C_8, C_{12}, C_{18}) have been reported as a function of the olefin length. The characteristics of the copolymers are given in table 1.

In the light of this information, we employed a coupling agent APTS in our study to prepare P(MA-*alt*-α-olefin)/SiO_2 hybrid materials with covalent bonds formed between organic and inorganic phases by an *in situ* sol–gel process of TEOS. Maleic anhydride-α-olefin copolymers reacted in the presence of APTS via the aminolysis reaction of anhydride groups and the amino groups of the coupling agent to generate covalent bonds between the copolymers and the inorganic precursor during the condensation step.

In situ formation of an inorganic network in the presence of preformed organic polymers was achieved to obtain nanohybrid structures having dual effect due to their polar and non-polar properties for the purpose of

Table 1. Intrinsic viscosities and molecular weights (GPC) of MA/α-olefins (C_6, C_8, C_{12}, C_{18}) copolymers.[15]

Copolymer	$[\eta]$	M_w	M_n	IP	Yield (%)
P(MA-HX)	0.0241	3750	2800	1.33	30
P(MA-OC)	0.0423	7300	5300	1.38	13
P(MA-DD)	0.0476	10700	7300	1.46	18
P(MA-OCD)[a]	0.1281	29600	12000	2.47	–

[a]Commercial sample, Aldrich Ltd.

generating a novel organonanofiller to be employed during the preparation of polymer-inorganic nanocomposites in reactive extruder systems. To attain our goal, interfacial interactions, silica network, thermal performance and morphology become highly important for the resulting polymer-inorganic hybrid materials and several complementary methods such as FTIR, ^{29}Si and ^{13}C–NMR, TGA, SEM and TEM have been used to characterize them.

2. Experimental

2.1 *Materials*

MA monomer (Aldrich, Germany) was purified before use by recrystallization from anhydrous benzene and sublimation under vacuum. α-olefins (C_6, C_8, C_{12},; Fluka, Switzerland) co-monomer was distilled under moderate vacuum before use. Benzoyl peroxide (BP; Fluka) was recrystallized twice from chloroform solution by methanol. Poly(MA-*alt*-1-octadecene) (C_{18}) was supplied from Aldrich with M_n = 30000–50000 g mol^{-1}. All other solvents and reagents were of analytical grade and used without purification. γ-Aminopropyltrimethoxysilane (APTS) and tetraethoxysilane (tetraethyl orthosilicate) (TEOS) were obtained from Aldrich and used as received.

2.2 *Measurements*

Fourier transform infrared (FTIR) spectra of the nanocomposites (KBr pellet) were recorded with an FTIR Nicolet 510 spectrometer in the 4000–400 cm^{-1} range, taking 30 scans at 4 cm^{-1} resolution. The solid-state NMR spectra were run at 75.5 MHz for ^{13}C and at 59.6 MHz for ^{29}Si on a Bruker Superconducting FT-NMR Spectrometer Avance with high power superconductive paramagnet TM 300 MHz WB in 7 mm MAS with a MAS angle of 54.7°. Thermogravimetric (TG) analysis was performed using a TA Instruments TA 2000 analyzer. Cured samples (50 mg) were analyzed in open (silicon) pans at 10°C /min in N_2 atmosphere up to a maximum temperature of 900°C. The structure of the samples was investigated by means of a FEI Tecnai G^2 Spirit Biotwin model High Contrast Transmission Electron Microscopy (CTEM) with Lantan Hexaboron Electron Gun. Copolymer/silica hybrid systems were studied at 120 kV. The suspensions of the powder samples were prepared in ethanol (0.5% w/w) and placed in ultrasonic bath for 20 min. 3–5 μL sample was dropped onto stabilized carbon coated Cu grids of 300 mesh and then allowed to dry. Samples for SEM analysis were sputter coated with Au/Pd using a Polaron SC7640 sputter coater. Scanning Electron Microscopy (SEM) images of the sample surfaces were obtained using an QUANTA 400F Field Emission SEM.

2.3 *Synthesis*

2.3a *Copolymerization of α-Olefins and Maleic Anhydride*: MA (0.017 mol), BP (4.05 mmol), and respective olefin (1-hexene, 1-octene, 1-dodecene) (0.204 mol) were added to a mixture of toluene (20 mL) and acetone (4 mL). The mixture was deaerated, filled with nitrogen and reacted at 70°C for 12 h. After solvent evaporation, the product was dissolved in toluene (7 mL) to separate all unreacted maleic anhydride, since this compound was insoluble in toluene. The polymer solution was then precipitated from hexane (75 mL), yielding a very fine white powder. The product was finally filtered, and dried for 6 h under reduced pressure.

2.3b *Preparation of Copolymer/Silica Hybrid Materials*: 1.4 mL of APTS/THF (1/9 V/V) mixture was added dropwise to 5 mL P(MA-*alt*-α-olefin)/THF (0.1 g/mL) solution under stirring for about 20 min (at APTS : MA mole ratio of 1:1), then 14.8 mL TEOS/THF (1/1 V/V) solution and 2.4 mL 0.14 mol/L HCl catalyst were added to the mixture obtained above under stirring for about 5 min. The transparent P(MA-*alt*-α-olefin)/silica hybrid materials were obtained upon gelling and drying at room temperature for about 3 weeks. Then the products were ground into fine powders. The products were finally vacuum dried for 6 h at room temperature.

3. Results and Discussion

In this study, the alternating copolymers of MA (electron acceptor monomer) with 1-hexene, 1-octene and 1-dodecene (electron donor monomers) were prepared (scheme 1) with the purpose of performing sol-gel reaction with TEOS in the presence of APTS to obtain poly(MA-*alt*-α-olefin)/SiO_2 hybrid structures. For comparison, a commercial sample of poly(MA-*alt*-1-octadecene) copolymer was also included.

3.1 *Interfacial Reactions-FTIR Studies*

The interfacial reactions between the coupling agent (APTS) and reactive copolymers were investigated by the comparative FTIR spectroscopic studies of copolymers and their prepared nanohybrids. The FTIR spectra of poly(MA-*alt*-α-olefin) copolymers and their nanohybrids are shown in figures 2 and 3, respectively.

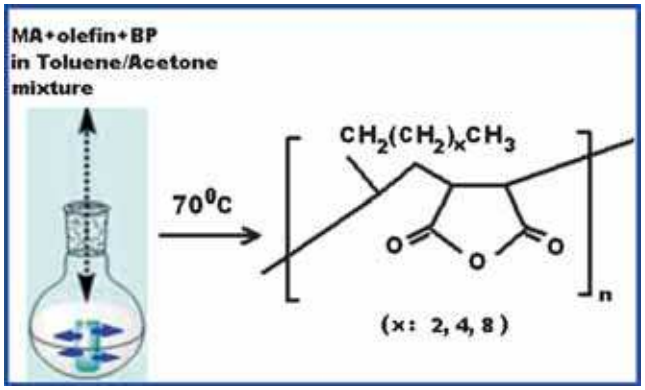

Scheme 1. Schematic representation of copolymerization of MA with 1-hexene, 1-octene and 1-dodecene.

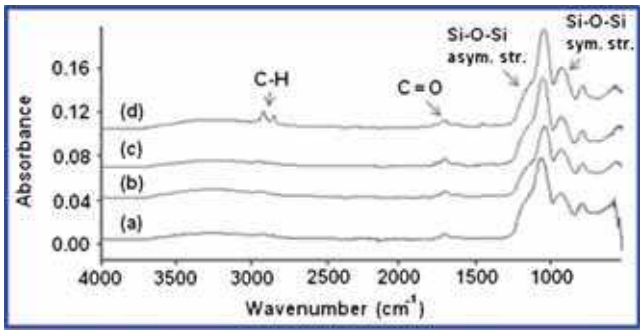

Figure 3. FTIR spectra of (a) poly(MA-*alt*-1-hexene)/SiO_2 nanohybrid, (b) poly(MA-*alt*-1-octene)/SiO_2 nanohybrid, (c) poly(MA-*alt*-1-dodecene)/SiO_2, and (d) poly(MA-*alt*-1-octadecene)/SiO_2 nanohybrid.

The analysis of the FTIR spectra allows us to reveal the following structural changes of macromolecules as a consequence of the intermolecular reactions between the functional groups of the copolymers and APTS (figures 2a and 3a) : (1) full disappearance of the anhydride unit band at 1847 and 1768 cm^{-1} ($\nu_{c=o}$); (2) appearance of N-H streching vibration bands in the range between 3600-3100 cm^{-1}; (3) appearance of Si-O-Si streching bands at 1039 cm^{-1}; (4) appearance of new absorptions around 1690 and 1700 cm^{-1}, corresponding to the C=O stretching vibration in amido and carboxyl groups, respectively. These indicate the formation of amide bonds due to the aminolysis of the maleic anhydride unit of copolymer with the coupling agent APTS during the synthesis of the hybrids. FTIR spectra of the latter three hybrids (figures 3b, c and d) are almost identical with that in figure 3a confirming nano level hybridization.

The decrease of the content of organic polymers would reduce the relative intensity of the carbonyl stretching vibration compared to that of Si–O–Si, regardless of the degree of hydrolysis. To obtain a precise degree of hydrolysis, the change in organic contents may be considered effectively. The intensity due to the carbonyl groups can be divided by the content of the organic elements in each hybrid and then the corrected values may well be used to determine the degree of hydrolysis. However, a more precise method, solid-state ^{29}Si NMR Spectroscopy has been employed in this study for confirming the degree of hydrolysis.

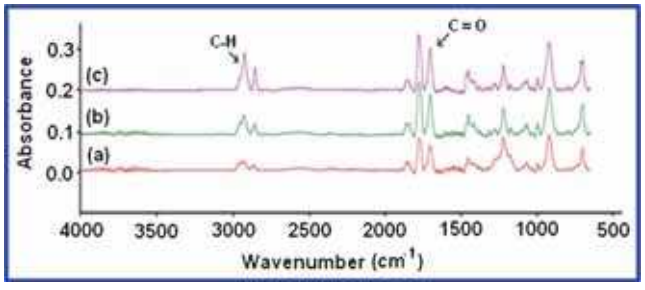

Figure 2. FTIR spectra of (a) poly(MA-*alt*-1-hexene), (b) poly(MA-*alt*-1-octene) and (c) poly(MA-*alt*-1-dodecene).

3.2 *Studying Sol-Gel Networks – ^{29}Si and ^{13}C CP MAS NMR Studies*

Insoluble or poorly soluble materials pose particular challenges to the analysis by NMR Spectroscopy because solubility is a strict requirement for the NMR studies. Besides, both macroscopic and microscopic parameters are influenced by the solution preparation process following chemical synthesis. This calls for powerful analytical tools that can probe these aspects in the material in solid state.[16] Owing to the presence of angular-dependent anisotropic interactions, the spectral resolution of solid-state NMR spectra is orders of magnitude lower than that of high resolution NMR in liquids. In principle, high-resolution solid-state NMR spectra can provide the same type of information that is available from corresponding solution NMR spectra, but special techniques/equipments are required, including magic-angle spinning (MAS), cross polarization (CP), etc.[17]

^{29}Si solid-state NMR gives further information on the structure of silica and the degree of Si-OH condensation reaction. In the ^{29}Si solid-state NMR spectra, peaks are generally denoted by the symbol Q^n to show un-, mono-, di-, tri-, and tetra-substituted siloxanes [$(RO)_{4-n}Si(OSi)_n$, R) H or an alkyl group]. For instance, a sample exhibiting a 100% Q^4 environment would possess a full condensed silica phase (i.e., corresponding to stoichiometric SiO_2). Such a deconvolution method

displays only semiquantitative results but enables comparison of samples with each other in terms of the condensation state of their silicate phases. The degree of condensation within the SiO_2 particles can be evaluated from the Q^4 percent.[18,19]

Sol-gel bonding in the synthesized four hybrid structures was studied with solid-state ^{29}Si NMR. Figure 4 displays the solid-state ^{29}Si MAS NMR spectra of the poly(MA-*alt*-α-olefin)/SiO_2 nanohybrid structures. The condensed siloxane species originating from TEOS, the silicon atoms through mono-, di- and tri- and tetra-substituted siloxane bonds were designated as Q^1, Q^2, $Q^3$and Q^4, respectively.

The γ-aminopropyltrimethoxysilane, APTS, similarly with mono-, di-, tri-, tetra-substituted siloxane bonds were designated as T^1, T^2, T^3, respectively. The various T^S are represented in figure 4 as an embedded scheme.[20]

Table 2. ^{29}Si MAS chemical shift assignments for silica[21,22] and synthesized copolymer-silica nanohybrids.

Samples	Silicon Atoms	Chemical Shift (ppm)	Content (%)
Silica	$Q^2[(Si\text{-}O)_2Si(O\text{-}H)_2]$	−91.2	–
	Q^3 $[(Si\text{-}O)_3Si\text{-}OH]$	−100.7	–
	$Q^4[Si(Si\text{-}O)_4]$	−111.3	–
P(MA-HX)/ SiO_2	$Q^2[(Si\text{-}O)_2Si(O\text{-}H)_2]$	−106	16.7
	Q^3 $[(Si\text{-}O)_3Si\text{-}OH]$	−115.3	54.2
	$Q^4[Si(Si\text{-}O)_4]$	−124.2	29.1
P(MA-OC)/ SiO_2	$Q^2[(Si\text{-}O)_2Si(O\text{-}H)_2]$	−105.3	9.1
	Q^3 $[(Si\text{-}O)_3Si\text{-}OH]$	−115.4	56.9
	$Q^4[Si(Si\text{-}O)_4]$	−123.8	34.0
P(MA-DD)/ SiO_2	$Q^2[(Si\text{-}O)_2Si(O\text{-}H)_2]$	−106.1	13.5
	Q^3 $[(Si\text{-}O)_3Si\text{-}OH]$	−115.4	51.0
	$Q^4[Si(Si\text{-}O)_4]$	−123.6	35.5
P(MA-OCD)/ SiO_2	$Q^2[(Si\text{-}O)_2Si(O\text{-}H)_2]$	−106.4	14.0
	Q^3 $[(Si\text{-}O)_3Si\text{-}OH]$	−114.9	60.9
	$Q^4[Si(Si\text{-}O)_4]$	−123.1	24.1

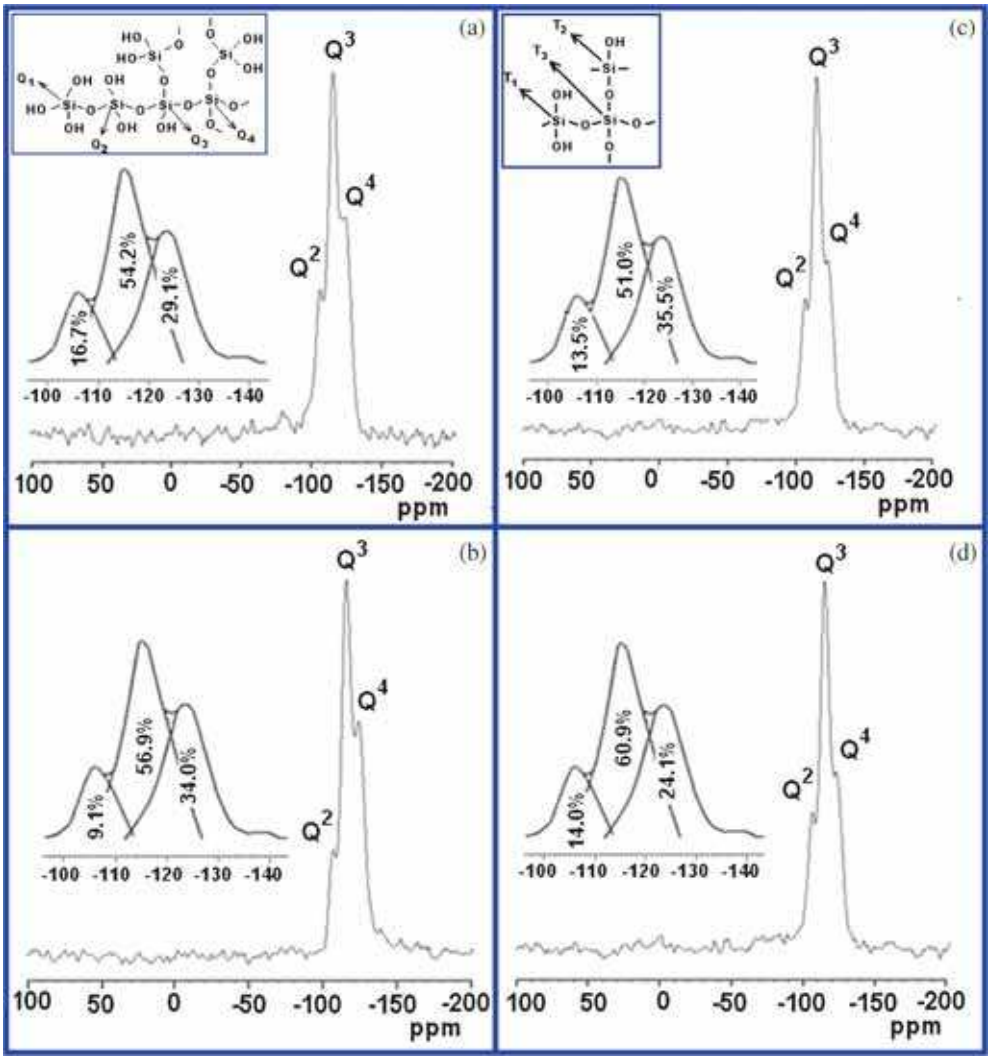

Figure 4. Solid-state ^{29}Si MAS NMR spectra of (a) poly(MA-*alt*-1-hexene)/SiO_2 nanohybrid, (b) poly(MA-*alt*-1-octene)/SiO_2 nanohybrid, (c) poly(MA-*alt*-1-dodecene)/SiO_2 nanohybrid, (d) poly(MA-*alt*-1-octadecene)/SiO_2 nanohybrid.

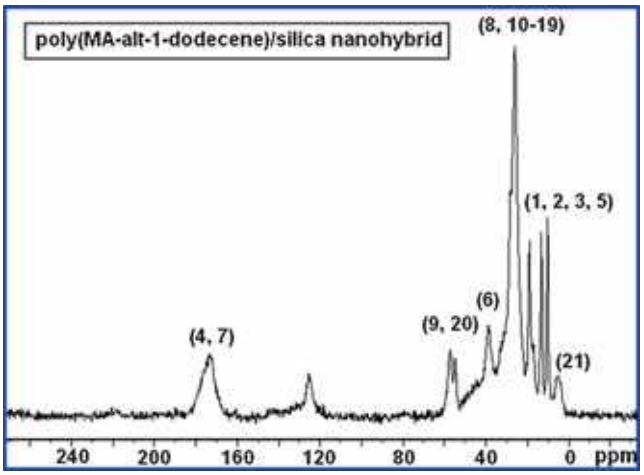

Figure 5. Solid-state ^{13}C CP/MAS NMR spectra of poly(MA-*alt*-1-dodecene)/SiO_2 nanohybrid.

The chemical shifts from the ^{29}Si NMR spectra of Q^2, Q^3, and Q^4 of four poly(MA-*alt*-α-olefin)/SiO_2 nanohybrids were determined and their peak areas were calculated (table 2) and these were similar to those reported in the literature.[21,22] Mono-substituted siloxane fragment is absent in the spectra, and condensation reactions via hydrolysis predominantly occur by the tri- and full-substitution with the formation of organo-silica nanoparticles covered with covalent bonding macromolecules of the alternating copolymer. Q^4 indicated complete silicon condensation, whereas, the existence of Q^3 and Q^2 reflected the incomplete condensation of TEOS. The characteristic chemical shifts of T^1, T^2 and T^3[23] are not taking part in the ^{29}Si NMR spectra of all samples. Results revealed that Q^3 and Q^4 were the major microstructures forming a network structure.

The degree of hydrolysis was also confirmed by solid-state ^{13}C CP/MAS NMR (figure 5). The peak for the carbonyl group was observed at 173 ppm while the peak for methine carbon at 57 ppm, the methylene carbon between 10-42 ppm and the methyl carbon at 5 ppm within the hybrid prepared in the presence of the acid catalyst. The peak at 57 ppm corresponded to the methylene carbon of the residual ethoxy group of TEOS. The methyl carbon was also diminishing. Again the result indicates that poly(MA-*alt*-1-dodecene) was effectively hydrolyzed in the silica matrix to afford a polymer hybrid.

In the light of FTIR, ^{29}Si and ^{13}C CP MAS NMR spectroscopic methods, a mechanism was proposed (figure 6) for the formation of organic/inorganic nanohybrids prepared by sol-gel reaction. Synthetic pathways for the preparation of poly(MA-*alt*-α-olefin)/SiO_2 nanohybrids can be displayed as follows:

With regard to the proposed mechanism, one can imply that the amino-group of the coupling agent (APTS) breaks the anhydride bond of maleic anhydride present in the copolymer structure to form carboxylic acid and amide. However, TEOS and triethoxy-silicon group of APTS form inorganic network by hydrolysis and condensation reactions, which can be demonstrated by the absorption peaks of Si–O–Si asymmetric stretching (~1100 cm^{-1}) and symmetric stretching (~820 cm^{-1}) with the corresponding chemical shift values (Q^2, Q^3, Q^4).

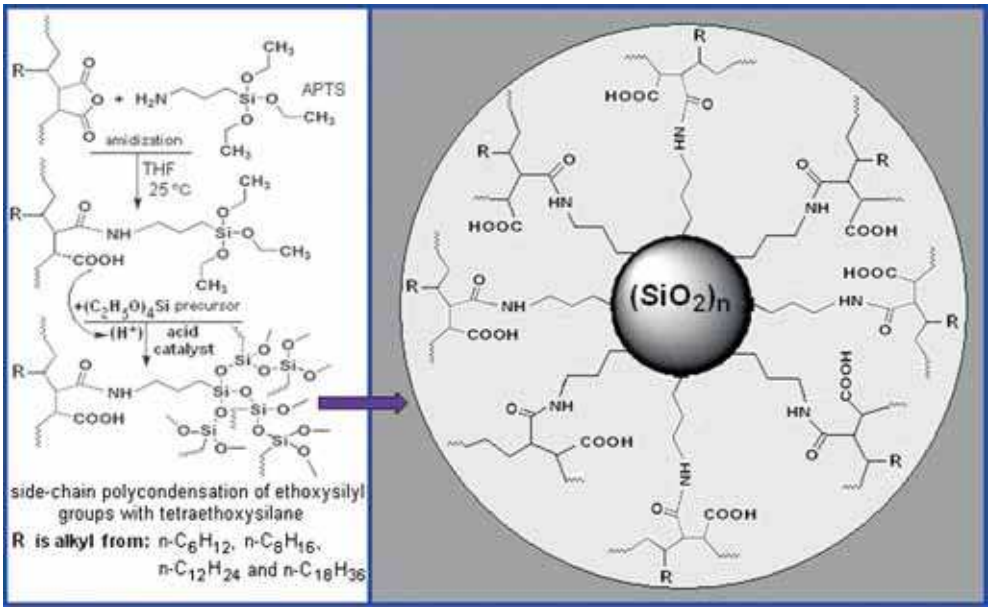

Figure 6. Proposed mechanism for the formation of organic/inorganic nanohybrids prepared by sol-gel reaction.

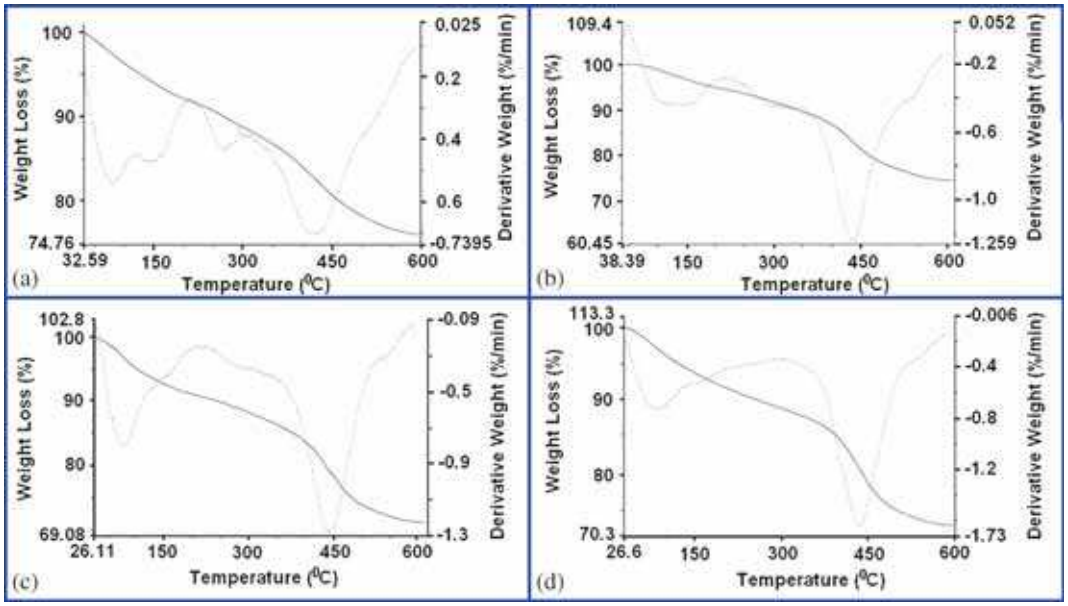

Figure 7. TGA thermograms and associated derivative curves of (a) poly(MA-*alt*-1-hexene)/SiO_2 nanohybrid, (b) poly(MA-*alt*-1-octene)/SiO_2 nanohybrid, (c) poly(MA-*alt*-1-dodecene)/SiO_2 nanohybrid, (d) poly(MA-*alt*-1-octadecene)/SiO_2 nanohybrid taken at a heating rate of 10°C/min under N_2.

3.3 *Thermal Degradation*

Figure 7 displays the thermogravimetric curves obtained from TGA and DTG thermograms of poly (MA-*alt*-α-olefin)/SiO_2 hybrids under nitrogen atmosphere at a heating rate of 10°C/min. In TGA thermogram of poly(MA-*alt*-1-hexene)/SiO_2 (figure 7a) a gradual weight loss of 8% of the original weight observed within the temperature range varying from 30°C to about 300°C can be reasonably attributed to the residual bonding of H_2O molecules and decarboxylation of anhydride units which are gradually volatilizing around that low temperature range.

Similar behavior was observed in the samples of poly (MA-*alt*-1-octene)/SiO_2, poly(MA-*alt*-1-dodecene)/SiO_2 and poly(MA-*alt*-1-octadecene)/SiO_2 at which the resulting weight loss percentages are 6, 9 and 11, respectively. However, in figures 7a and b, there is a dramatic appearance of a peak between 150-300°C corresponding to CO_2 elimination resulting from decarboxylation process. This peak gradually decreases in figure 7c and finally disappears in figure 7d. This means that the copolymer hybrids with shorter alkyl side chains would be less stable than those with longer ones. In other words, longer alkyl chains would probably be protecting the carboxylic residue. In this way, this group would be less exposed to thermal decomposition. In DTG curve (figure 7a) a strong narrow peak at 424°C refers to main chain scission within the copolymer, implying that thermal degradation of the corresponding hybrid starts at this point. In table 3, the

Table 3. Thermal parameters and percent silica contents of pristine copolymers and resulting hybrid structures.

System	$T_{1-onset}$	T_d(°C)	$T_{2-outset}$	Silica content (weight %)
P(MA-HX)	302	395	501	–
P(MA-OC)	305	398	506	–
P(MA-DD)	305	400	509	–
P(MA-HX)/SiO_2	350	424	590	70
P(MA-OC)/SiO_2	370	433	595	75
P(MA-DD)/SiO_2	365	438	580	76
P(MA-OCD)/SiO_2	360	436	575	73

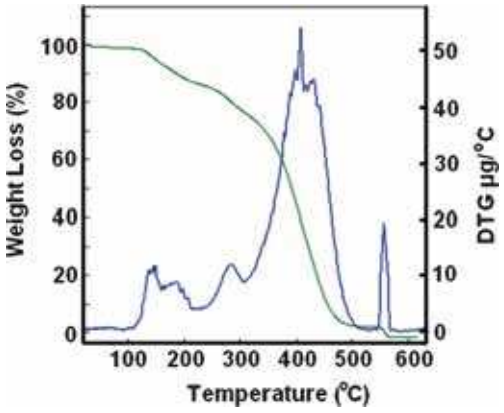

Figure 8. TGA thermograms and associated with DTG curves of pristine poly(MA-*alt*-1-dodecene) taken at a heating rate of 10°C/min under N_2.

corresponding degradation temperatures of the other samples are presented. Additionally, another shorter peak range between 450-550°C with the variation of samples is observed, which may be due to the degradation of the SiO_2 network or to the main chain that binds silica to the polymer by a covalent bond directly.

Thermogram for thermal degradation of pristine poly(MA-*alt*-1-dodecene) is shown in figure 8. The thermal degradation of each hybrid structure starts at a higher temperature ($T_{1-onset}$) when compared with that of pristine copolymers as shown in table 3. It is normally expected that the thermal stability of the polymer hybrid should be higher when compared with that of the individual polymer. Further, it is assumed that the rigid siloxane matrix surrounds the organic polymer by molecular level hybridization, which influences the enhancement of thermal stability of the hybrid[24] to higher extents. This is due to the fact that the plasticizing trimethoxysilyl groups have transformed to silica network during the sol-gel process. The large-scale cooperative movement of the polymer chain segments (i.e., glass transition) was highly restricted by the crosslinking points that are generated from the formation of covalent bonds between the polymer chains and the silica network as well as by steric hinderance of the rigid silica (hydrolysis and condensation of TEOS) framework.[20]

The weight residue remaining at 600°C was regarded as the real silica content. The percent silica incorporated in the polymer matrix is given in table 3.

It is difficult to decide whether the thermal behavior changes of nanohybrids occur due to the variation of long and branched alkyl chains or not. It must be considered that the molecular weight of these copolymers is not identical. Besides, the decarboxylation degree and silica % are also effective on T_d value. The most crucial evaluation is the significant increase in T_d values for the obtained hybrids when compared to that of pristine copolymer.

3.4 *SEM studies of the copolymer/silica hybrid materials*

SEM studies were carried out for the observation of microstructural details and characterization of the topmost surface composition of the obtained copolymer-silica hybrids on a nanometer scale.

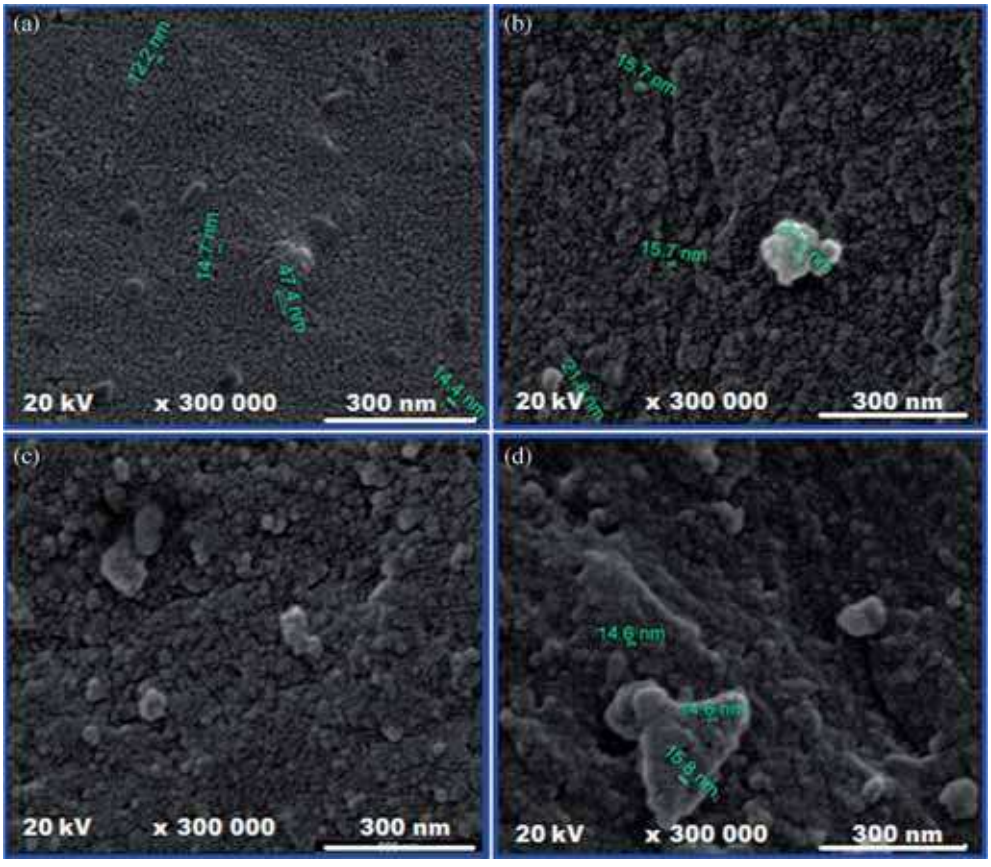

Figure 9. SEM images of (A) poly(MA-*alt*-1-hexene)/SiO_2, (B) poly(MA-*alt*-1-octene)/SiO_2, (C) poly(MA-*alt*-1-dodecene)/SiO_2 and (D) poly(MA-*alt*-1-octadecene)/SiO_2.

From figure 9, it can be seen that the SiO_2 particles were smaller than 50 nm indicating that the prepared hybrid materials could be regarded as nanohybrids and and size distributions are narrow. The uniform dispersion of silica in the copolymer/SiO_2 nanohybrids indicate that silica networks were restrained under molecular level in the nanohybrids. The good distribution and small size of silica particles in hybrids mainly resulted from the strong interaction between polymer and silica through coupling agents. In all the samples the silica particles are spherical in shape.

There is also agglomeration between spherical silica nanoparticles leading to large size particles causing the scatter of the light and resulting in the opaqueness of the hybrids. However, this reveals that the size of inorganic particles is no more than 50 nm. Some irregular particles with a wide size distribution are observed. This suggests that there are two populations of particles, which accompany agglomeration of individual particles. The size of individual particles is much smaller than that of the agglomerates. Large particles may be caused by hydrophobic agglomeration at long and branched alkyl groups in copolymer or by hard agglomeration during drying. In figures 9 (A) to (D), respectively, the effect of long and branched alkyl groups in nanocomposites can be clearly observed. The tendency of these groups towards agglomeration is visibly increased by increasing alkyl chain length.

3.5 *TEM studies of the copolymer/silica hybrid materials*

Controlling the morphology of particles is very important to master their physicochemical properties. This study involves successive steps to establish a physicochemical or chemical link at the interface of the organic and inorganic constituents: (i) the selection of copolymers containing functional ingredients of polymerization, namely, the surfactant, the monomer, as poly(MA-alt-α-olefin)s, (ii) obtaining the template for nanoparticles with *in situ* sol-gel process by using TEOS as an inorganic precursor in the presence of APTS as coupling agent.

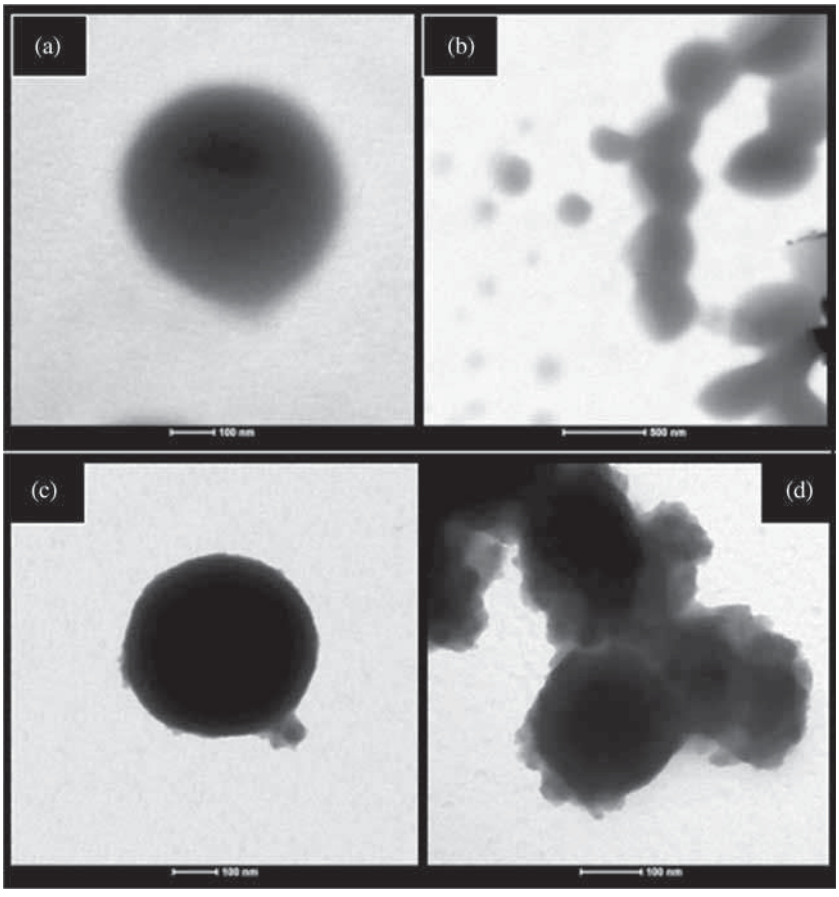

Figure 10. High Contrast TEM images of poly(MA-*alt*-1-hexene)/SiO_2; (a) at 100 nm, (b) 500 nm and poly(MA-*alt*-1-octene)/SiO_2; (c) and (d) at 100 nm from different regions.

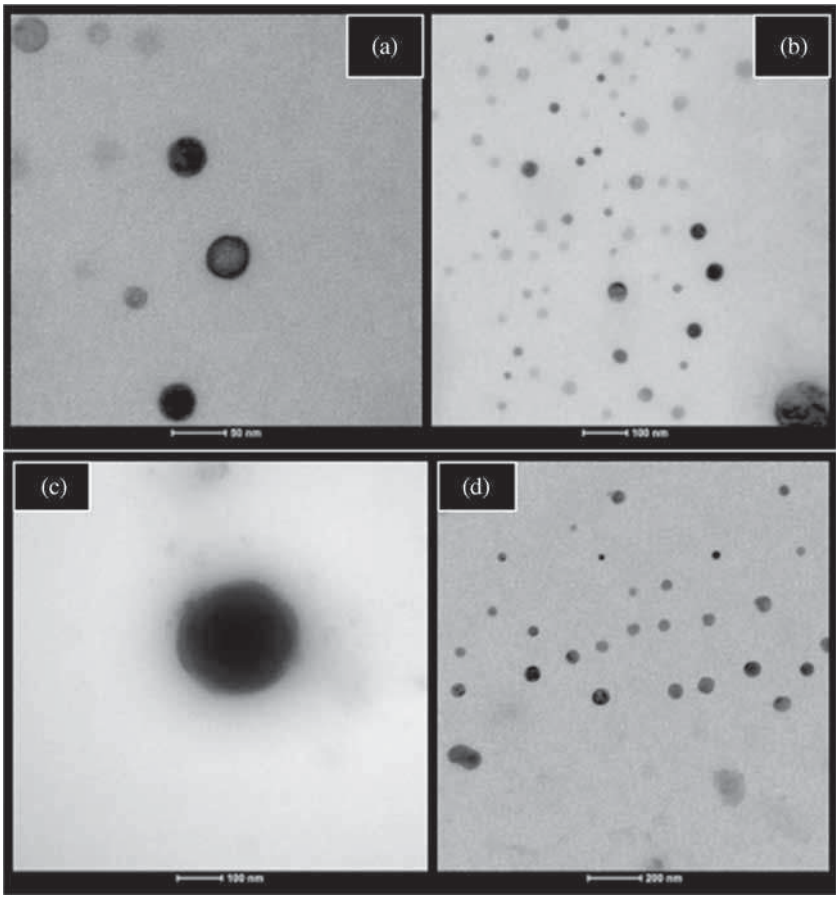

Figure 11. High Contrast TEM images of poly(MA-*alt*-1-dodecene)/SiO_2; (a) at 50 nm, (b) 100 nm and poly(MA-*alt*-1-octadecene)/SiO_2; (c) at 100 nm and (d) 200 nm from different regions.

Figures 10 and 11 show the TEM micrographs of poly(MA-*alt*-α-olefin)/silica nanohybrids. The copolymer/silica nanohybrids have spherical morphology. On an average the interparticle distance as well as the polymer–silica interaction are high in all samples. However, silica aggregates still would lead to voids in between silica particles. Consequently, solvent will easily penetrate into these voids where polymer–solvent interactions play an important role.

In this work, we report a facile *in situ* surfactant-free method to synthesize poly(MA-*alt*-α-olefin)/silica nanohybrids since the self percolation without using any surfactant is possible due to the surfactant property of the long and branched alkyl group bearing copolymer itself. With regard to the percolation phenomena, once the distance between the nanoparticles gets close to double of the "real radius", the nanoparticles form an interconnected network, which is called "rheological percolation".[25] As a result of nucleation of individual nanoparticles, the formed nanoparticle complex is actually larger than the radius of the bare nanoparticles.

4. Conclusions

Alternating copolymers of maleic anhydride (MA) with α-olefins (C_6, C_8, C_{12}) prepared by free radical copolymerization reaction and another copolymer of MA with a higher α-olefin (C_{18}) (obtained commercially) were employed for the purpose of obtaining poly(MA-*alt*-α-olefin-C_6, C_8, C_{12}, C_{18})/SiO_2 nanohybrids. These nanohybrids with covalent bonds between organic and inorganic phases were successfully prepared by *in situ* sol-gel process with TEOS in the presence of APTS. Poly(MA-*alt*-α-olefin) copolymers were incorporated into an inorganic network through the aminolysis reaction of the MA units of the copolymer with the coupling agent APTS.

Sol-gel networks and interfacial interactions in these hybrid systems were revealed by spectroscopic studies (FTIR and ^{29}Si MAS NMR). Appearance of Si-O-Si band in FTIR spectra accompanied by the appearance of representative peaks at characteristic chemical shift values (Q^2, Q^3, Q^4) in ^{29}Si MAS NMR spectra indicates a silica network formation. The peaks in the

range between 3600-3100 cm^{-1} (N-H stretching) and the peaks around 1690 and 1700 cm^{-1} (C=O stretching vibration inamido and carboxyl groups) appeared simultaneously with full disappearance of the peaks at 1847 and 1768 cm^{-1} (anhydride unit band) corresponding to the breakage of amide bonds following the aminolysis reaction occurring at themaleic anhydride unit of the copolymer with the coupling agent APTS during the synthesis of the hybrids.

SEM results confirm the uniform distribution and the small size of silica particles in hybrids mainly resulting from the strong interaction between the copolymer and silica through the selected coupling agent. Inorganic phases have a small size referred to nanohybrids. The TEM results allowed us to propose a morphological scheme for each hybrid. The systems exhibit spherical morphology with regard to the chosen matrix copolymers which contain both hydrophobic, long and branched alkyl fragments and hydrophilic anhydride groups. Common particle-matrix morphology, where silica particles tend to form aggregates in the continuous copolymer phase, can be considered as nanohybrid materials.

The hybrids have new nanosystems with extremely good heat resistance when compared with that of pristine copolymers. It can be concluded that the properties of these materials are not only due to the sum of individual contributions of both phases, but also due to the role of the interfaces which could be predominant.

References

1. Xanthos M 2005 In *Functional Fillers for Plastics* (Weinheim: Wiley-VCH Verlag)
2. Yiu-Wing M and Zhong-Zhen Y 2006 In *Polymer nanocomposites*, (Boca Raton: CRC Press)
3. Jothibasu S, Kumar A A and Alagar M 2007 *J. Sol-Gel Sci. Technol.* **43** 337
4. Yuan Q W and Mark J E 1999 *Macromol. Chem. Phys.* **200** 206
5. Nass R 1990 *J. Non-Crystalline Solids* **121** 370
6. Sarwar M I and Ahmad Z 2000 *Europ. Polym. J.* **36** 89
7. Zhao Z D, Gao Z M, Ou Y C, Qi Z N and Wang F 1996 *Acta Polym. Sin.* **2** 228
8. Hasegawa N, Kawasumi M, Kato M, Usuki A and Okada A 1998 *J. Appl. Polym. Sci.* **67** 87
9. Kawasumi M, Hasegawa N, Kato M, Usuki A and Okada A 1997 *Macromolecules* **30** 6333
10. Manias E, Touny A, Wu L, Strawhecker K, Lu B and Chung T C 2001 *Chem. Mater.* **13** 3516
11. Bozdoğan D D, Kibarer G and Rzayev ZM O 2011 *I. RE. CH. E.* **4** 232
12. Rzaev Z M O 2000 *Prog. Polym. Sci.* **25** 163
13. Nagasawa M and Price S 1960 *J. Am. Chem. Soc.* **80** 5070
14. Frank H P 1968 *Macromol. Chem. Phys.* **114** 113
15. Marti'nez F, Uribe E and Olea A F 2005 *J. Macromol. Sci. Part A Pure Appl. Chem.* **42** 1063
16. Nishijima Y 1970 *J. Polym. Sci. Polym. Symp.* **31** 353
17. G Kickelbick (Ed.) 2007 In *Hybrid materials. Synthesis, characterization, and applications* (Weinheim, Germany: Wiley-VCH)
18. Hajji P, David Gerard J F, Pascault J P and Vigier G 1999 *J. Polym. Sci. Part B: Polym. Phys.* **37** 3172
19. Gao Y, Choudhury N R, Dutta N, Matisons J, Reading M and Delmotte L 2001 *Chem. Mater.* **13** 3644
20. Da Z L, Zhang Q Q, Wu D M, Yang D Y and Qiu F X 2007 *Express Polym. Lett.* **10** 698
21. Qiu F X, Jiang Y, Zhou Y M and Liu J Z 2006 *Silicon Chemistry* **3** 65
22. Bauer F, Ernst H, Decker U, Findeisen M, Glasel H J, Langguth H, Hartmann E, Mehnert R and Peuker C 2000 *Macromol. Chem. Phys.* **201** 2654
23. Joseph R, Zhang Z and Ford W T 1996 *Macromolecules* **29** 1305
24. Liu P and Su Z 2004 *Mater. Chem. Phys.* **94** 412
25. Jiahua Z, Suying W, Yutong L, Luyi S, Neel H, Young D P, Cara S, Airat K, Zhiping L and Zhanhu G 2011 *Macromolecules* **44** 4382